ISSN 8755-6839

SCIENCE OF TSUNAMI HAZARDS

Journal of Tsunami Society International

Volume 34 Number 3 2015

# NUMERICAL SIMULATION OF UJONG SEUDEUN LAND SEPARATION CAUSED BY THE 2004 INDIAN OCEAN TSUNAMI, ACEH-INDONESIA

**Musa Al'ala[1, 3], Syamsidik[3, 4], Teuku Muhammad Rasyif[2, 3], and Mirza Fahmi[2,]**

1 Student at Civil Engineering Department, Syiah Kuala University, Jl. Syeh Abd. Rauff, No.7, Banda Aceh, 23111 Indonesia.
2 Post graduate student at Civil Engineering Master Program, Syiah Kuala University, Jl. Syeh Abd. Rauff, No.7, Banda Aceh, 23111. Indonesia.
3 Tsunami and Disaster Mitigation Research Center, Syiah Kuala University, Jl. Prof. Ibrahim Hasan, Gampong Pie, Banda Aceh, 23233 Indonesia.
4 Civil Engineering Department, Syiah Kuala University, Jl. Syeh Abd. Rauff, No. 7, Banda Aceh, 23111, Indonesia.
musaalala@gmail.com

**ABSTRACT**

The Aceh province in Indonesia, located around the Sumatra subduction area, was one of the worst hit areas with respect to damage from the impact of the 2004 Indian Ocean tsunami. A 9.15 Mw earthquake triggered the tsunami. One of the impacts was the disconnection of several areas from their mainland, thus creating new small islands. This happened around Ujong Seudeun village in Aceh Jaya District. Prior to the tsunami, the village had approximately 500 residents. However, after the tsunami, the area was severely eroded and a small strait had been inserted between the village and the Sumatra Island mainland. This study investigates the magnitude of the tsunami wave forces that separated the area to yield a newly deserted small island. This study was conducted by numerical simulations and by coupling the COMCOT (Cornell Multi-grid Coupled Tsunami Model) and Delft3D models. These tools have specific advantages, namely, COMCOT's linear modeling is based on a series of earthquake mechanisms and Delft3D uses non-linear morphological dynamic modeling. Their software includes the explicit leapfrog finite difference scheme (COMCOT) and the non-linear shallow water equation (Delft3D). Bathymetry data from

newly formed coastline and the small island's shape were digitized using 2005 Quickbird Images. Results from this research reveal the estimated tsunami wave heights and forces that disconnected the small island of Ujong Seuden from the Sumatra Island mainland. These results can be used to further develop the COMCOT model to incorporate sediment modules.

**Keywords:** *morphology, erosion, and tsunami wave height, COMCOT, Delft3D.*

## 1. INTRODUCTION

The Aceh province in Indonesia, located around the Sumatra subduction area, was one of the worse areas with respect to damage from the impact of the 2004 Indian Ocean tsunami. A 9.15 Mw earthquake triggered the tsunami. One impact was the disconnection of several areas from their mainland to create small islands such as those around the village of Ujong Seudeun. This village is located in Aceh Jaya District near the Geurutee mountainside. Before the tsunami, this village had approximately 500 residents, but today, this village has no permanent residents. Locals now utilize this area solely for beef husbandry and coconut farming. Ujong Seudeun is now constrained by the massive sediment transport that caused the land separation. With respect to impact of tsunami waves on sediment transport, the tsunami deposit has generated a lot of research interest (Dawson et al. 1996; Moore et al. 2007; Shi et al. 1995; Gelfenbaum and Jaffe 2003; Richmond et al. 2012). Studies have focused on determining how the tsunami made its impact and how the hydrodynamic forces worked to separate the land bar. For time and efficiency considerations, numerical simulations are required to investigate these phenomena. The research based on numerical simulation with respect to combine tsunami propagation and sediment transport is rarely and it still needs some improvement. This paper is aimed at investigating the process of the land separation due to the tsunami wave forces by means of numerical simulations'. The tsunami waves propagation and sediment transport produced during the propagation can be analyzed with numerical modeling. The tsunami waves propagation can been conducted using COMCOT (Cornell Multi- grid Coupled Tsunami Model) (Liu et al., 1994; 1998). To simulation near shore process including sediment transport, Delft3D-FLOW developed by Deltares (2007) of the Netherland offers some advantages. In this study, tsunami propagation is simulated with COMCOT using the leap-frog finite difference based on a series of earthquake mechanisms. The COMCOT results are then used as input for a sediment transport simulation using Delft3D-FLOW and its non-linear shallow water equation. The result would appeal the process of the sediment transport coupled with Delft3D-FLOW in producing close fitted result from COMCOT tsunami propagation. This paper provides the first physical explanation ever on the creation of a new Island of Ujong Seudeun in Aceh after the 2004 Indian Ocean tsunami.

## 2. STUDY AREA

Ujong Seudeun is an area in Aceh Jaya, near the Geurutee mountainside. Located between 5.116847° N and 95.294216° E, Ujong Sedeun is 75.1 km from Banda Aceh, the capital city of the Aceh province. Prior to the tsunami, this area had approximately 500 residents and had an infrastructure, including a mosque and houses. Since the tsunami hit Aceh, following the 2004 megathrust earthquake, Ujong Seudeun has been deserted. Because the land connectin Ujong Seudeun with the main island was swept away, its residents were forced to move to the main island. A 1519-m-long area eroded after the tsunami, leaving Ujong Seudeun completly separated

from the island. The tsunami wave and natural interventions since that time have transformed 1,538,854 $m^2$ of land into ocean (according to shoreline comparations on Google Earth images taken on June 23, 2003 and March 2, 2011).

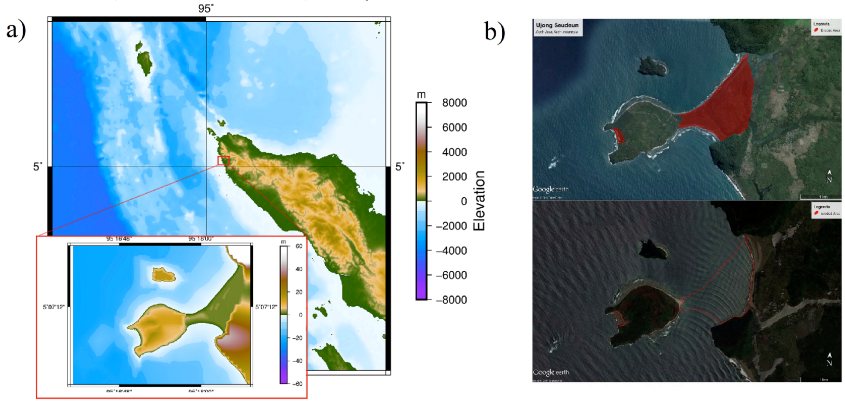


Figure 1. (a) Ujong Seudeun on Sumatra Island and (b) Ujong Seudeun area before and after the 2004 Indian Ocean Tsunami by Google Earth image.

## 3. METHOD

First, we began the numerical simulation process by preparing the data for layer setup. We used General Bathymetric Chart of the Oceans (GEBCO) data for the larger grid (layers 1 and 2), and for layers 3 and 4, we used GEBCO data with a smaller grid size and updated it with available navigation charts. We used a multi-fault machanism developed by Romano (2009) and employed these data to run a 3-hour COMCOT simulation. We then analyzed the hydrodynamic data produced by the COMCOT simulation to determine the shear stresses that had occurred. The simulation was then continued for the sediment transport process using Delft3D-FLOW as it also has been helpful for the tsunami propagation (Vatvani et al., 2012). In addition, we used the hydrodynamic data from the fourth layer elevation data as input for Delft3D-FLOW.

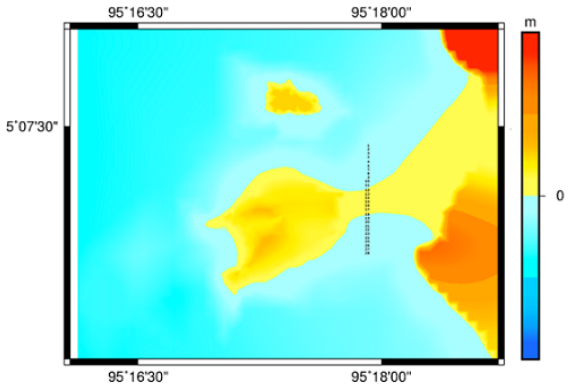


Figure 2. Layer 4 with 28 observation points.

Hydrodynamic forces affect the water depth and area characteristics. To investigate the operation of these forces, we applied data from 28 observation points located across the land bar area in the COMCOT simulation, as shown in Figure 2. Each observation point was 50 m long. In addition, we applied 4 other observation points at each edge of the water area in layer 4. These extra observation points provided water depth and depth-averaged velocity data for the Delft3D-FLOW input, as boundary data. Observation points were also applied in the Delft3D-FLOW simulation to record the sediment transport process that occurred.

### 3.1 Fault Model

The 2004 megathrust earthquake located at 95.8° E and 3.4° N resulted in significant dislocation. The earthquake occurred at 07:59 am local time and within 8 to 10 min caused ruptures to the western coast of northern Sumatra Island as far as 1200–1300 km from the Andaman–Sunda Sea. The complex fault mechanism of the rupture process is difficult to explain. To describe the complexity of the multi-fault mechanism, several researchers have proposed earthquake source parameters. In this research, we used the multi-fault mechanism developed by Romano (2009). This model was also used by Liu et al. (2012) to investigate the morphological changes in Aceh from the 2004 tsunami. As explained by Okada (1985), tsunamis are generated by the deformation of the sea floor, which is instantly reproduced at the sea surface. This theory is also known as the deformation model.

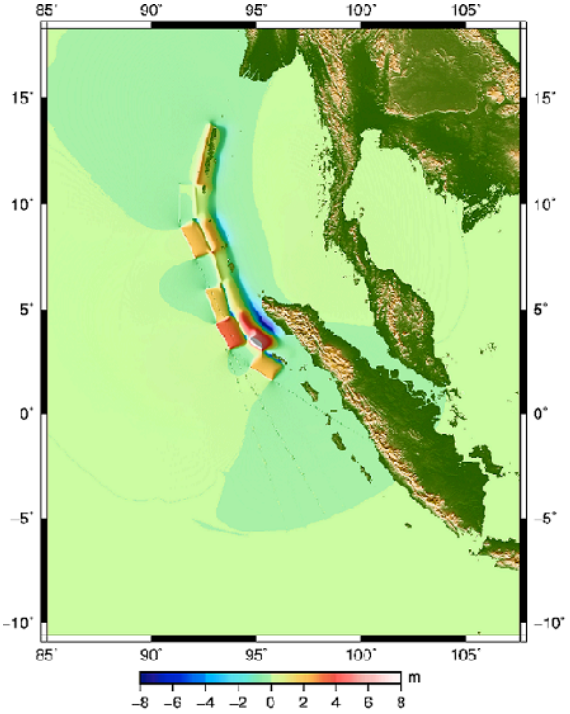


Figure 3. Initial condition and earthquake epicenter for 2004 tsunami.

### 3.2 Grid Set up

We performed the numerical simulation using an equation that could process a large amount of data. A dynamic coupled system of nested grids was employed to simulate the tsunami propagation from the Andaman–Sumatra subduction zone toward the location under consideration (Wang and Liu, 2008). COMCOT uses a nested grid system with 4 layers of different size and resolution and has its own shallow water equation (linear or non-linear). In the first layer, we used GEBCO data with a grid resolution of 1 min (1851 m), and the rupture area was located in the simulation area. Almost identical to the first layer, we also used GEBCO data in layer 2, interpolated into a 0.1667-min grid (308.5 m).

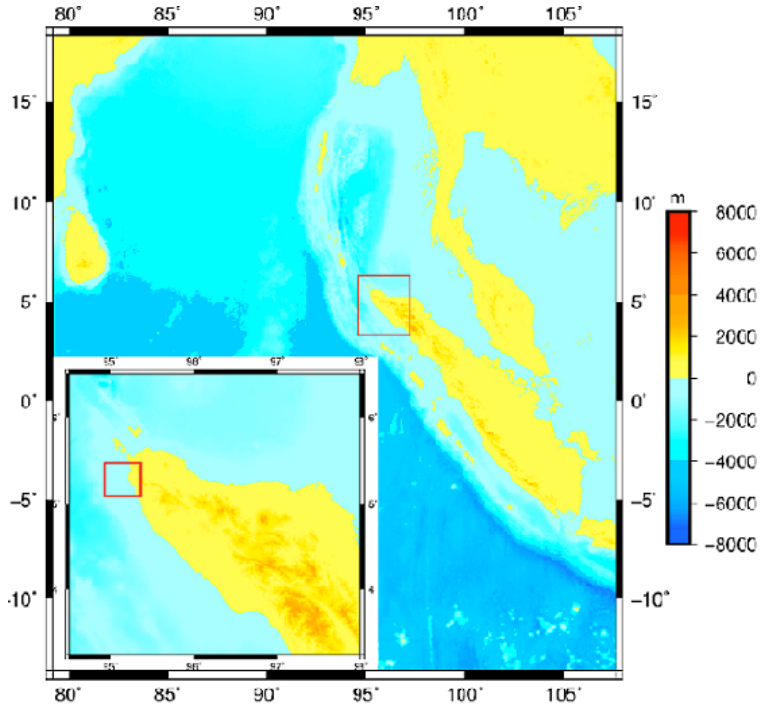


Figure 4. Layer 1 of computational domain with layer 2 marked in a red rectangle.

Next, layer 3 was interpolated into a 0.0277-min grid from ETOPO2 data and updated with a navigation chart from DISHIDROS TNI AL (Indonesian Marine Corps). This chart covers depths of 3000–4000 m at a 1:100000 scale. The fourth layer was treated in almost the same way as layer 3, but in a different area and to a different extent. This layer was interpolated into a 0.0048-min grid from ETOPO3 and was updated with other navigation chart data to replace the GEBCO land elevation data used prior to its erosion.

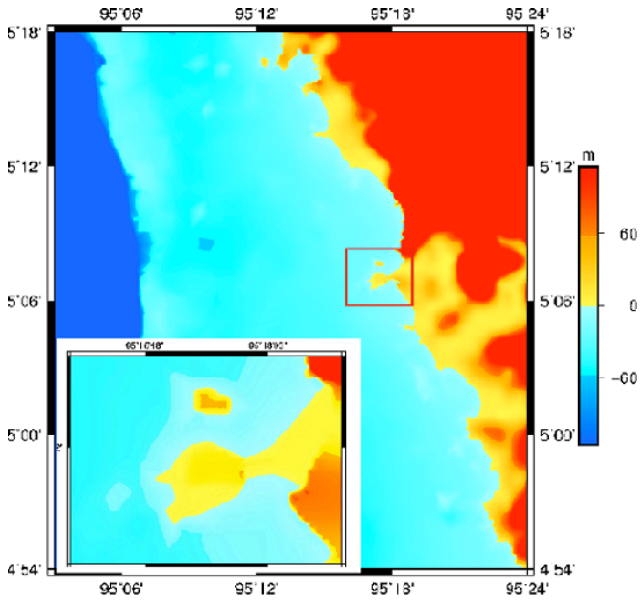


Figure 5. Layer 3 of computational domain with layer 4 marked in a red rectangle.

**TABLE 1.** Grid specifications for each layer.

| Layer Id | extent of grid Longitude | Grid Spacing | Grid size and coordinate system | Grid size and coordinate system | Type of Shallow water equation |
|---|---|---|---|---|---|
| Layer 01 | 79.2–107.6 | −13.6–18.1833 | 1 min (1851 m) | 1705 × 1908 Spherical | Linear |
| Layer 02 | 94.61–97.79 | 3.41–6.29 | 0.166 min (307.266 m) | 1146 × 1038 Spherical | Linear |
| Layer 03 | 95.053–95.50 | 4.803–5.247 | 0.0277 min (51.27 m) | 966 × 960 Spherical | Linear |
| Layer 04 | 95.269–95.310 | 5.102–5.134 | 0.00463 min (8.76 m) | 534 × 414 Spherical | Linear |

### 3.3 Numerical Simulation

Numerical simulation was performed with COMCOT to simulate the tsunami propagation. We used the leap-frog finite difference scheme in the nested grid system to calculate both shallow

water equations (linear and non-linear). This model has been validated experimentally (Liu et al., 1995) and has been successfully implemented to investigate historical tsunami events such as the 1992 Flores Island tsunami (Liu et al., 1995) and the 2004 Indian Ocean tsunami (Wang and Liu, 2006a, 2006b, 2007).

In the nested grid system, the inner grid is adapted to a smaller size and nested inside an outer grid. Water elevation and depth-averaged velocity results are then interpolated from the larger grid into the smaller one. The larger grid contains layers 1, 2, and 3, and we used the linear shallow water equation for the grid system. Layer 4 differs from the other three layers as it comparatively smaller in size. The governing equations in the cartesian coordinate system of the non-linear shallow water equation that we used can be expressed as follows:

$$\frac{\partial \eta}{\partial t} + \frac{1}{R\cos\varphi}\left\{\frac{\partial P}{\partial \psi} + \frac{\partial}{\partial \varphi}\left(\cos\varphi Q\right)\right\} = -\frac{\partial h}{\partial t}, \quad (1)$$

$$\begin{aligned}&\frac{\partial P}{\partial t} + \frac{1}{R\cos\varphi}\frac{\partial}{\partial \psi}\left\{\frac{P^2}{H}\right\} + \frac{1}{R}\frac{\partial}{\partial \varphi}\left\{\frac{PQ}{H}\right\}, \\ &+ \frac{gH}{R\cos\varphi}\frac{\partial \eta}{\partial \psi} - f Q + F_x = 0\end{aligned} \quad (2)$$

$$\begin{aligned}&\frac{\partial Q}{\partial t} + \frac{1}{R\cos\varphi}\frac{\partial}{\partial \psi}\left\{\frac{PQ}{H}\right\} + \frac{1}{R}\frac{\partial}{\partial \varphi}\left\{\frac{Q^2}{H}\right\}, \\ &+ \frac{gH}{R}\frac{\partial \eta}{\partial \varphi} + f P + F_y = 0\end{aligned} \quad (3)$$

$$f = \Omega \sin\varphi \quad , \quad (4)$$

$$F_x = \frac{gn^2}{H^{7/3}} P\left(P^2 + Q^2\right)^{1/2} \quad , \quad (5)$$

$$F_y = \frac{gn^2}{H^{7/3}} Q\left(P^2 + Q^2\right)^{1/2} \quad , \quad (6)$$

$$H = \eta + h \quad , \quad (7)$$

where $\eta$ is the water surface elevation; $(P, Q)$ gives the volume fluxes in $X$ (west–east) direction and $Y$ (south–north) direction, respectively; $(\varphi, \psi)$ are the latitude and longitude; $R$ is the Earth's radius; $g$ is the gravitational acceleration; and $h$ is the water depth. The term $-\partial h/\partial t$ reflects the effect of transient seafloor motion; $f$ represents the Coriolis force coefficient due to the Earth's rotation; $\Omega$ is the rotation rate of the Earth; $H$ is the total water depth; $F_x$ and $F_y$ represent the bottom friction in the $\psi$ and $\varphi$ direction, respectively; and $n$ is Manning's roughness coefficient.

## 4. RESULTS

The hydrodynamic forces were produced with the COMCOT simulation, which made it possible to consider the tsunami wave height and depth-averaged velocity. Furthermore, these two factors were used as input to calculate shear stress in the inundation area. The next step in the investigation of how the tsunami impact caused the land separation required the simulation of the sediment transport. Tsunami wave height was used as input data for Delft3D-FLOW. The morphological change was simulated by Delft3D-FLOW in 1 hour.

### 4.1 Tsunami Hydrodynamic

Land separation is caused by a number of hydrodynamic forces, including wave height and depth-averaged velocity. Wave heights were massively dispersed until reaching and inundating the land area, and they severely impacted the sediment transport by erosion and sedimentation. The COMCOT simulation results showed that the wave height at observation point 15 reached 16.054 m. This result clearly demonstrates the occurrence of overtopping in the Ujong Seudeun land bar area that connected the village to the main island.

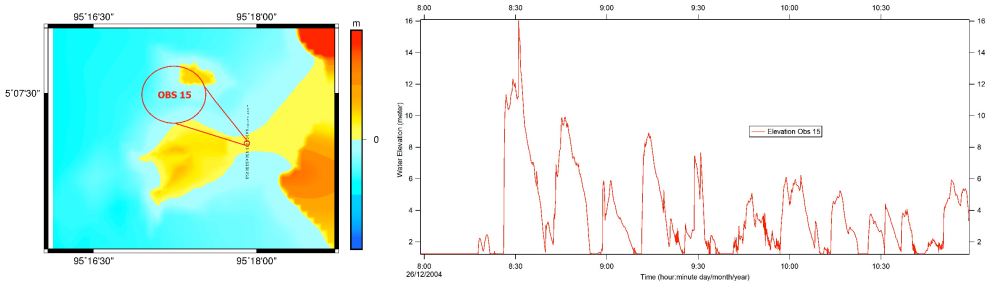


Fig 6

Overtopping occurred over a 3-hour duration in the COMCOT simulation. The highest wave came within 24 min at a height of 16.054 m, as shown in Figure 6. This event made the highest impact on the sediment transport, and the others followed to complete the hydrodynamic process. The shape of the area contributed to the overall impact, since waves that came into the area near the land bar observation point were narrower.

The COMCOT simulation results show the average maximum tsunami wave height at each observation point to be 15 m. This simulation result clearly explains how overtopping occurred numerous times since the highest elevation in the land bar area was only 4.6 m high.

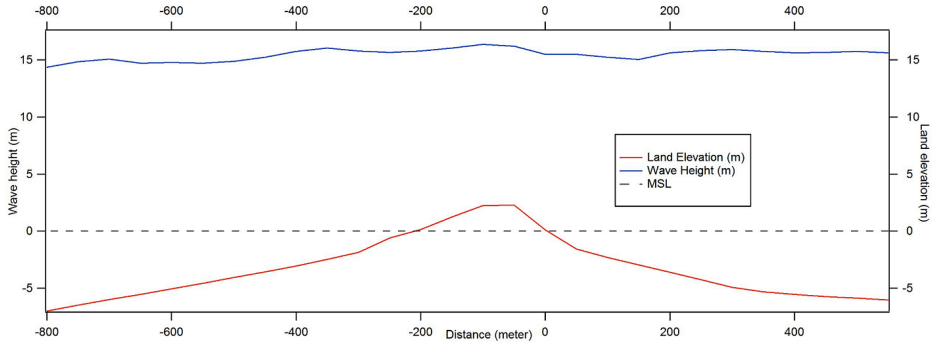


Figure 7. Maximum wave height at each observation point.

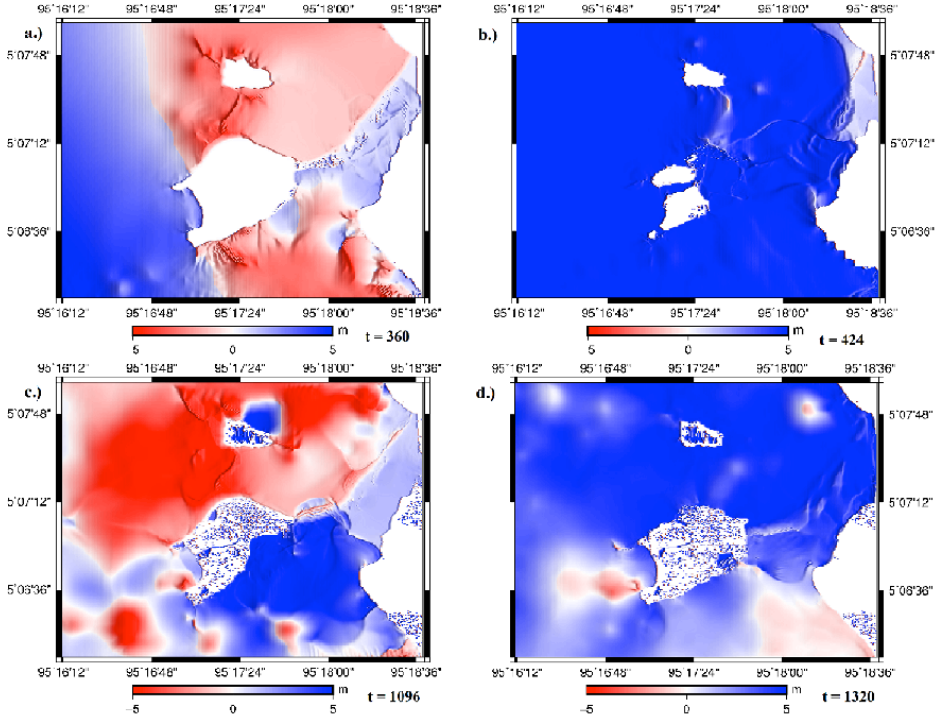


Figure 8. Tsunami dispersion in COMCOT simulation.

Tsunami waves overtopped the land several times in the COMCOT simulation, with the first wave hitting the western area of Ujong Seudeun 6 min after the earthquake. Although these first waves hit and flooded the land bar area, their impact was not great because their heights did not

reach 1 m. After 1 min and 4 sec, the waves coming from the west direction turned north on the upper side of the land bar and turned south on the lower side. As the waves met at the land bar, they merged into a higher wave but did not cause the land bar to separate from the mainland, as shown in Figures 8(a) and 8(b).

As the simulation process continued, we observed the wave suspected to have eroded the land area at 18 min and 16 sec after the megathrust earthquake. The wave came from the south of Ujong Seudeun Island and struck the land bar. At this point, the land bar began to erode but not significantly. It then continued to erode, and sediment was deposited at different locations and times. In addition, the depth-averaged velocity was high, as derived from the COMCOT simulation, with most of the wave reaching 10 m/s, and the highest velocity occurring at observation point 19 with 10.930 m/s. This high velocity contributed to the generation of a high bed shear stress, which then led to a greater capability for the flow (tsunami wave) to erode the sediment particles. Depth function is a significant aspect of the shear stress calculation, such that the shear stress produced in shallow water is bigger than that in deep areas. The depth-averaged velocity also plays an important role. It increased in the area near the land bar because the cross-section area had become smaller. The flow continued through with the same volume but through a narrower area.

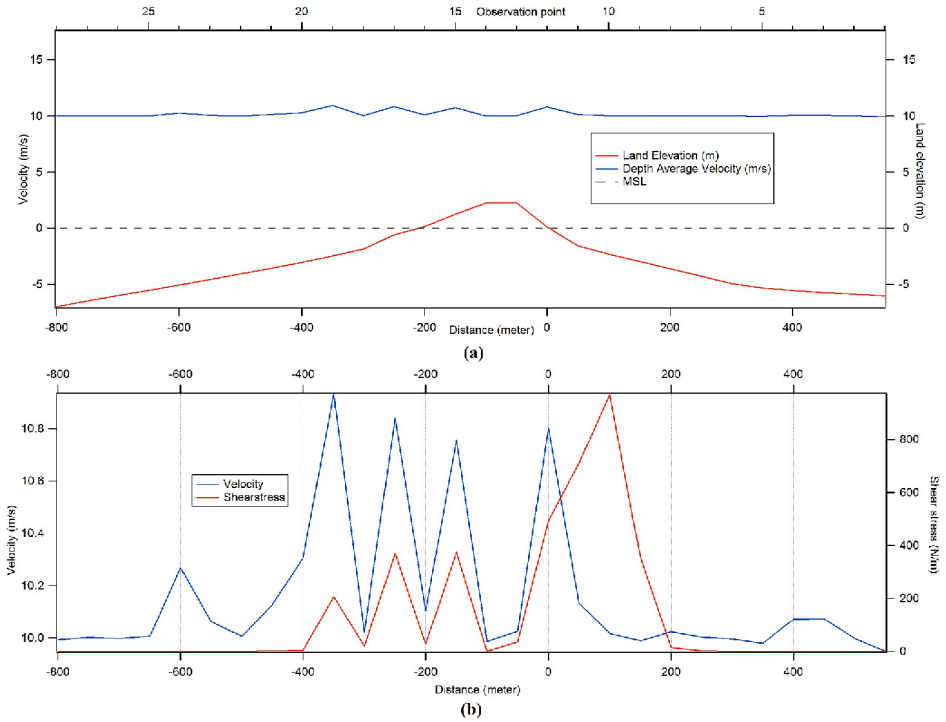


Figure 9. (a) Maximum tsunami height and (b) maximum velocity with shear stress at several observation points.

The shear stress results graphed in Figures 9(a) and 9(b) show the velocity and shear stress fluctuations and illustrate the sediment transport process as it occurred. The fluctuations of these two parameters indicate the high probability for the Ujong Seudeun land bar to be eroded and ultimately swept away. This hypothesis is confirmed in the sediment transport subsection.

### 4.2 Sediment Transport

Sediment transport requires hydrodynamic forces capable of moving sediment particles. A significant change in water elevation will produce a strong and high velocity that will affect particle movement on the sea bed. Tsunami waves produce a massive volume of sea water by changing the characteristics of an area, consequently generating a high and variable depth velocity. The depth velocity produced in the 2004 Indian Ocean tsunami was high enough to make a huge impact, affecting wave heights and water volumes, as well as the bathymetry. As happened in Ujong Seudeun, the COMCOT simulation results show that wave heights reached 16.054 m, which is more than sufficient to significantly impact the sediment transport process.

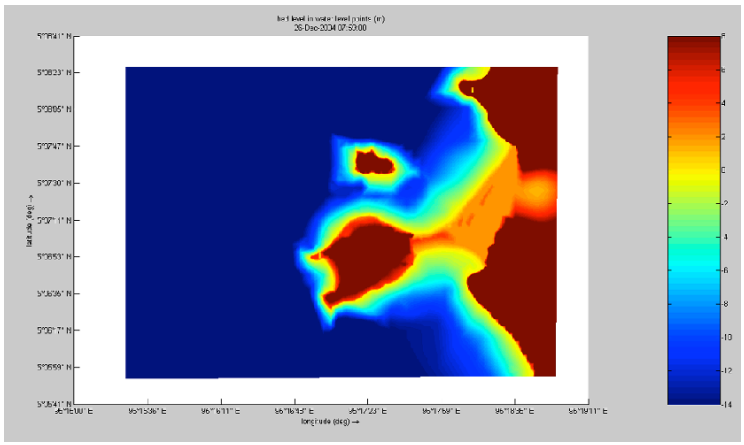

Figure 10. Simulation area on Delft3D-FLOW.

We used Delft3D-FLOW to simulate the sediment transport process during a 1-hour tsunami simulation using COMCOT layer 4, as shown in Figure 10. The hour-long Delft3D_FLOW sediment transport simulation showed very clearly that the land bar was eroded due to the tsunami waves. We ran the Delft3D-FLOW simulation using COMCOT's tsunami waves and layer 4 elevation as input data.

The Delft3D-FLOW simulation results were nearly identical to those of the COMCOT simulation. The real erosion impacts, as seen in the COMCOT simulation, started 21 min after the simulation began (at 08:22 am local time). The wave came from the north and seemed like a back wave from the northern area because the rupture sources were from the western area. The waves were continuous until the land bar completely separated after 44 min (08:43 am local time). Waves that came from the south, west, and north brought a high speed current that caused sedimentation

and erosion in some areas and at various times. Elevation changes were recorded by the observation points on the land bar in the Delft3D simulation process. There were 14 observation point on the land bar area, but only five were used to represent the sediment transport process, including obs 5, 6, 11, 12, and 13.

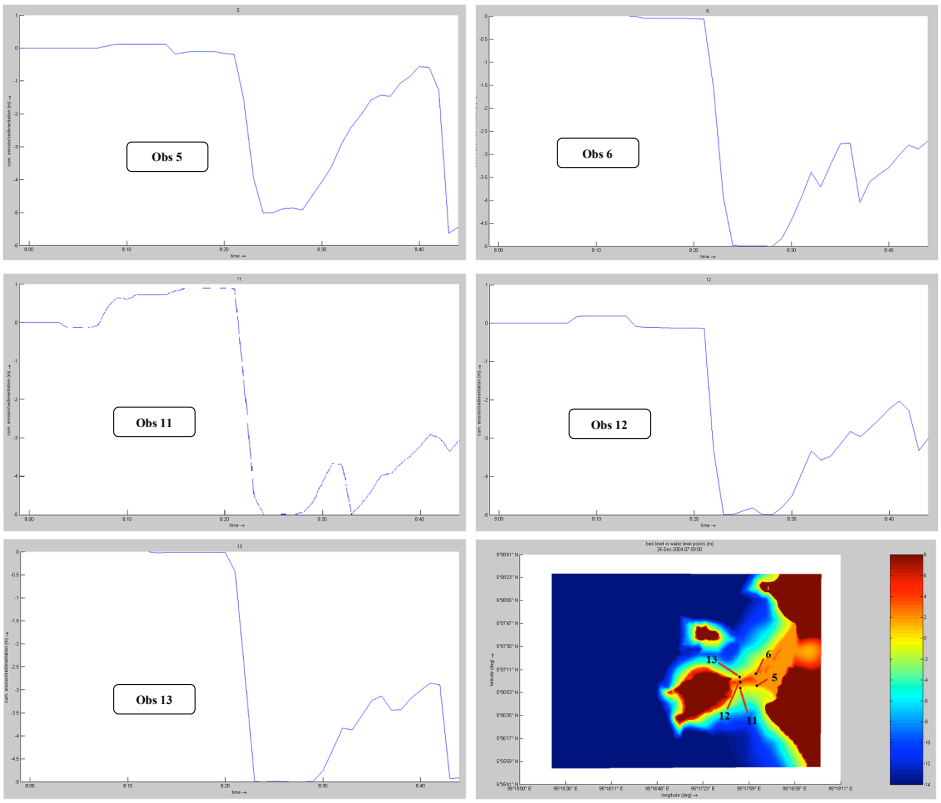


Figure 11. Simulation graphic of sediment transport process at several represented observation points.

The sediment transport process revealed by these 5 observation points represents the erosion process as observed by Delft3D. Each of the observation points illustrate the sediment transport accumulation process, and all five observation points show that the erosion process began 22 min after the earthquake. The tsunami waves continuously eroded the land bar and produced an area averaging 3.2 m in depth. This happened because the beach morphology and Keluwang Island near Ujong Seudeun trapped the waves and amplified their effect. The amplification became sufficiently large to erode the entire land bar area and leave Ujong Seudeun as a completely separate island in Aceh Jaya.

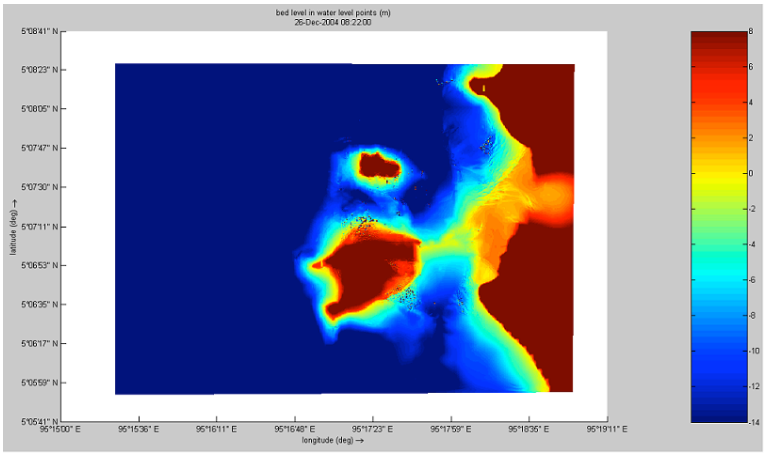


Figure 12. Simulation area 23 min after hit by tsunami wave.

Author 6/5/15 7:57 AM
**Comment:** Remark: Please verify if this should be 22 min.

## 5. CONCLUSIONS

The efficient investigation of the land separation impacts of a tsunami (sediment transport process) requires a numerical simulation approach. In this study we observed two events—the tsunami propagation and the sediment transport process. We simulated these two events continuously using two different software tools. The tsunami propagation was simulated with COMCOT and the sediment transport process was simulated with Delft3D-FLOW. The COMCOT simulation was performed with GEBCO data and available navigation charts, and the simulation results were then used as input data for Delft3D-FLOW to observe the sediment transport prosess on the land bar that connected Ujong Seudeun to the main island. The COMCOT simulation results show that the tsunami waves had a massive impact on the land separation in Ujong Seudeun. This impact was confirmed by the Delft3D-FLOW simulation results. The land bar that connected Ujong Seudeun with the main island began to erode 22 min after the earthquake occurred, and it separated completely after another 22 min. These processes explained the tsunami's huge impact on the erosion of the land until it separated as well as how the separation occurred. These results also demonstrate that COMCOT and Delft3D-FLOW can be coupled to model tsunami sediment transport.

## ACKNOWLEDGMENTS

The authors are grateful to USAID and the National Academy of Sciences who funded this research through PEER Cycle 3, Sponsor Grant Award Number: AID-OAAA-A-11-00012 and Sub Grant Number PGA-2000004893 with the research project title: Tsunami Waves Impacts on Coastal Morphological Changes Based on Sediment Transport Simulations.

**REFERENCES**


1. Deltares (2007) Deltares, User Manual Delft3D-Flow: Simulation of Multi-Dimensional Hydrodynamic Flows and Transport Phenomena, Including Sediments (Delft, The Netherlands).
2. Jaffe B, Gelfenbuam G (2007) A simple model for calculating tsunami flow speed from tsunami deposits. Sediment Geol 200(3–4):347–361
3. Moore A, Nishimura Y, Gelfenbaum G, Kamataki T, Triyono R (2006) Sedimentary deposits of the 26 December 2004 tsunami on the northwest coast of Aceh, Indonesia. Earth Planets Space 58(2):253–258
4. Richmond B, Szczucin´ski W, Chague´-Goff C, Goto K, Sugawara D, Witter R, Tappin DR, Jaffe B, Fujino S, Nishimura Y, Goff J (2012) Erosion, deposition and landscape change on the Sendai coastal plain, Japan, resulting from the March 11, 2011 Tohoku-oki tsunami. Sediment Geol 282:27–39.
5. Shi S, Dawson AG, Smith DE (1995) Coastal sedimentation associated with the December 12th, 1992 tsunami in Flores, Indonesia. Pure and Applied Geophysics 144(3–4):525–536
6. Vatvani, D., Van Veen, B. A. D. And Zijl, F (2012) Tsunami flood modeling for Aceh and West Sumatra and its application for an early warning system. Continent. Shelf Res.
7. Wang, X., Liu, Philip L-F (2006a) An analysis of 2004 Sumatra earthquake fault plane mechanisms and Indian Ocean tsunami. Journal of Hydraulic Research 44 (2):147–154
8. Wang, X, Liu, Philip L-F (2006b) The 2004 Indian Ocean Tsunami: Inundation Simulation at Trincomalee, Sri Lanka, Internal report (Personal communication)
9. Wang, X, and Liu, Philip L-F (2007) Numerical simulations of the 2004 Indian Ocean tsunamis: coastal effects. Journal of Earthquake & Tsunami 1(3):273–297
10. Borsje, B.W. et al., Modeling large-scale cohesive sediment transport affected by small-scale biological activity, Estuar. Coast.Shelf Sci. (2008), doi:10.1016/j.ecss.2008.01.009